

## Resistivity Structure of the Showa-Shinzan Dome at Usu Volcano, Hokkaido, Japan

Yoshihiko GOTO\* and Akira JOHMORI\*\*

(Received October 30, 2013; Accepted January 18, 2014)

A controlled source audio frequency magnetotelluric (CSAMT) survey was conducted over Showa-Shinzan Dome at Usu Volcano, Hokkaido, Japan, in order to investigate its internal structure. The Showa-Shinzan Dome (800–1000 m across, 350 m high) is a partly extruded cryptodome that formed in AD 1943–45 due to the uplift of pre-existing rocks and sediments by the intrusion of dacitic magma. The dome comprises a flat-topped cryptodome called ‘Yaneyama’ and a dacitic lava dome projecting above the Yaneyama cryptodome. The CSAMT survey was carried out on a 1600-m-long line that crosses the Showa-Shinzan Dome in an east-west orientation. Two-dimensional inversion of the CSAMT data revealed the resistivity structure at depths less than 1000 m beneath the dome. The resistivity structure suggests the existence of a sub-spherical dacite intrusion (resistivity  $50\text{--}130\ \Omega\cdot\text{m}$ ;  $\sim 400$  m across) below the summit of the Showa-Shinzan Dome. The dacite intrusion may represent the solidified dacitic magma emplaced in AD 1943–45. The Yaneyama cryptodome only comprises pre-existing rocks and sediments uplifted by the intrusion of dacite magma. The upper zone of the Yaneyama cryptodome consists of the Usu Somma Lava ( $> 100\ \Omega\cdot\text{m}$ ), whereas the lower zone consists of Quaternary pyroclastic flow deposits and sedimentary rocks ( $< 30\ \Omega\cdot\text{m}$ ), such as the Toya pyroclastic flow deposits, the Fukaba Formation, the Takinoue welded tuff, the Sobetsu pumice flow deposits, and the Yanagihara Formation. There is no dacite intrusion beneath the Yaneyama cryptodome. This structural model is consistent with the distribution of active fumaroles on the Showa-Shinzan Dome, and also with historical records of dome growth. The geophysical data provide new insights into the formation mechanism of the Showa-Shinzan Dome.

**Key words:** resistivity survey, CSAMT method, Showa-Shinzan Dome, internal structure, Usu Volcano

### 1. Introduction

Resistivity surveying provides valuable information on the underground geological structures of active volcanoes (e.g., Aizawa *et al.*, 2008, 2009; Aizawa, 2010; Fikos *et al.*, 2012; Matsushima *et al.*, 2001; Nishida *et al.*, 1996; Ogawa *et al.*, 1998; Risk *et al.*, 2003; Srigutomo *et al.*, 2008; Yamaya *et al.* 2009). We have conducted a controlled source audio frequency magnetotelluric (CSAMT) survey (Milsom, 2003; Sandberg and Hohmann, 1982) of the Showa-Shinzan Dome of Usu Volcano, Hokkaido, Japan, in order to investigate its internal structure. The Showa-Shinzan Dome is a partly extruded cryptodome formed in AD 1943–45 due to the uplift of pre-existing rocks and sediments by the intrusion of dacitic magma (Katsui, 1988; Mimatsu, 1962; Minakami *et al.* 1951; Soya *et al.*, 2007; Yokoyama *et al.*, 1973). The internal structure of this dome has previously been studied using various geophysical techniques, including seismology (Kato and Shoji, 1949; Hayakawa *et al.*, 1957; Nemoto *et al.*, 1957), magnetic surveying (Nishida and Miyajima, 1984), and

muon radiography (Tanaka *et al.*, 2007; Tanaka and Yokoyama, 2008), but still remains poorly constrained. Herein, we present the results of a CSAMT survey of the Showa-Shinzan Dome and discuss the nature of the subsurface geology beneath the dome.

### 2. Showa-Shinzan Dome

The Showa-Shinzan Dome is located at the eastern foot of Usu Volcano (Fig. 1). The dome is elliptical in plan view with a diameter ranging from 800 m (N-S) to 1000 m (E-W), and it rises 350 m above the surrounding area (Fig. 2). The highest point of the dome is 398 m above sea level. The dome consists of a flat-topped cryptodome called ‘Yaneyama’ and a pyramidal dacitic lava dome projecting above the Yaneyama cryptodome (Fig. 2A).

The Yaneyama cryptodome is pancake-shaped, 800–1000 m across, and 200 m thick. The surface of the cryptodome mainly comprises andesitic lava blocks (2–5 m in size) of the Usu Somma Lava (Yokoyama *et al.*, 1973) and unconsolidated sediments (soil, clay, and volcanic ash) that

\* College of Environmental Technology, Graduate School of Engineering, Muroran Institute of Technology, Mizumoto-cho 27-1, Muroran, Hokkaido 050-8585, Japan

\*\* Neo Science Co. Ltd, Tarui 4-2-30, Sennan, Osaka 590-

0521, Japan

Corresponding author: Yoshihiko Goto  
e-mail: ygoto@mmm.muroran-it.ac.jp

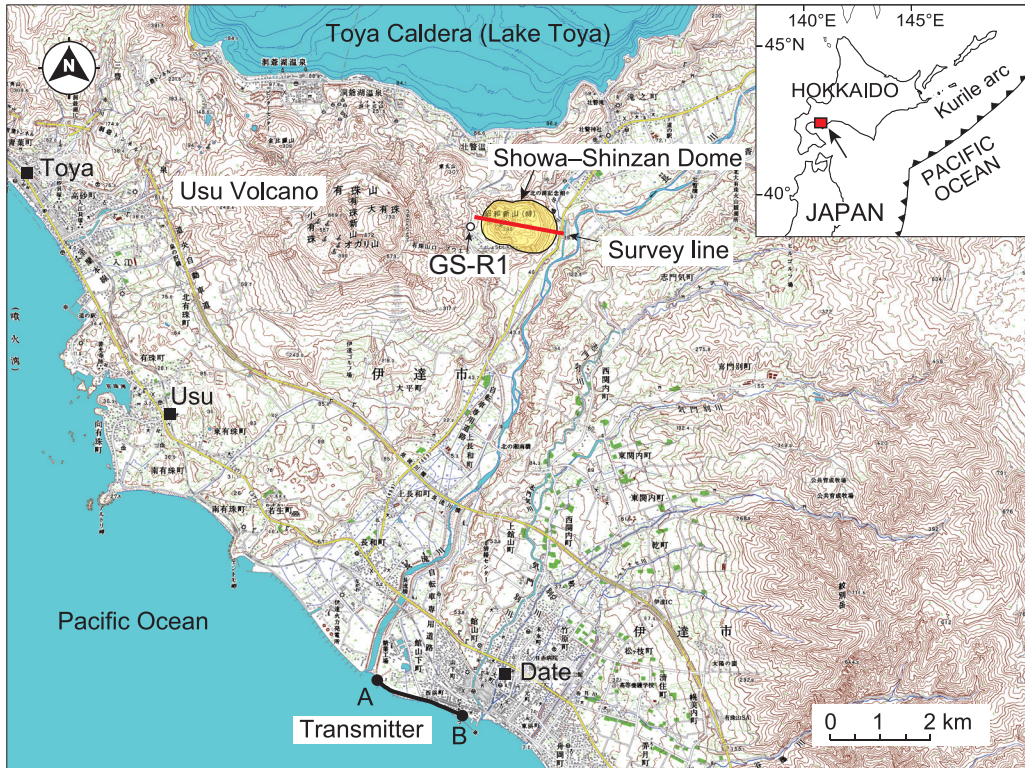


Fig. 1. Location map of the Showa-Shinzan Dome (yellow area) in the eastern part of Usu Volcano, southwestern Hokkaido, Japan. Also shown is the location of the CSAMT survey line (red line). The points marked A and B are the ends of the grounded wire (dipole source) of the transmitter for the CSAMT survey (black line). Location of the GS-R1 hole (see Fig. 8) is also shown. The base map was taken from the 1 : 50,000 scale topographic maps ‘Toyako-onsen’ and ‘Date’ issued by the Geospatial Information Authority of Japan. The topographic contour interval is 20 m.

were uplifted during dome growth. The geology of the interior of the Yaneyama cryptodome is poorly understood due to dense vegetation cover (Fig. 2B) and the absence of cross-sectional exposures. The Yaneyama cryptodome hosts no active fumaroles, apart from the region in the immediate vicinity of the lava dome (Symonds *et al.*, 1996).

The dacitic lava dome projects from the western side of the Yaneyama cryptodome (Fig. 2A). The dome has a pointed top and steeply sloping sides, and is 300–400 m in diameter and rises 150 m above the Yaneyama cryptodome. The lava dome consists of fresh coherent dacite ( $\text{SiO}_2 = 69 \text{ wt.}\%$ ; Oba *et al.*, 1983) that contains phenocrysts of plagioclase and hypersthene. Most of the lava dome is covered with reddish brown, clayey rocks (‘natural brick’; Mimatsu, 1962) that were formed by the heating of uplifted sediments in contact with hot dacitic magma. The lava dome hosts a number of active fumaroles (Symonds *et al.*, 1996) and its surface is almost bare (Fig. 2B).

Minakami *et al.* (1951) and Mimatsu (1962) documented that the formation of the Showa-Shinzan Dome

was preceded by a series of severe earthquakes on 28 December 1943. In January 1944, the ground at the eastern foot of Usu Volcano began to inflate and many cracks opened in the ground. On 23 June 1944, the first phreatic explosion took place in this area, and explosions repeatedly occurred until October 1944. By late October, the amount of inflation had reached 150 m, thereby forming a flat-topped cryptodome (Yaneyama). In November 1944, a dacitic lava dome was extruded upwards on the western side of the Yaneyama cryptodome and was accompanied by further growth of the Yaneyama cryptodome. The growth of the lava dome continued until September 1945.

### 3. CSAMT survey

The CSAMT survey was performed in order to obtain a resistivity structure at depths of up to 1000 m beneath the Showa-Shinzan Dome. The survey was carried out on an east-west line passing over the Yaneyama cryptodome and the lava dome (Fig. 3). The CSAMT survey was performed following the ‘scalar CSAMT’ method (Matsuoka, 2005; Yokokawa, 1984; Fig. 4), whereby a transmitter injects

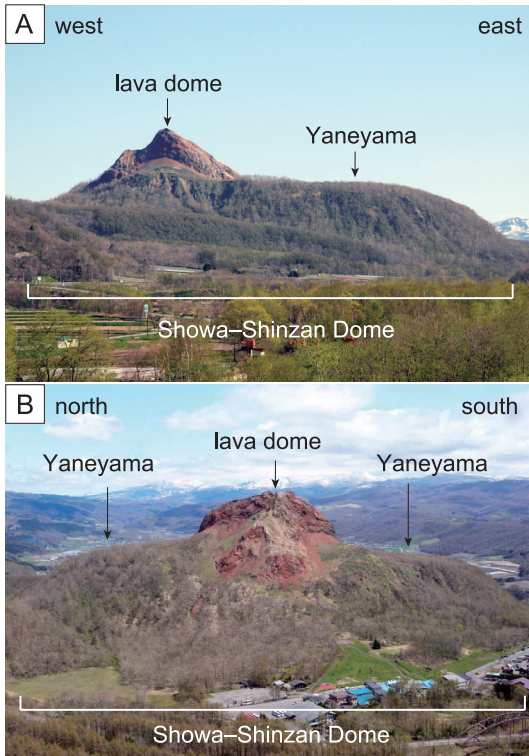


Fig. 2. Photographs of the Showa–Shinzan Dome viewed from the south (A) and west (B). The dome consists of a flat-topped cryptodome named ‘Yaneyama’ and a pyramidal dacitic lava dome projecting above the Yaneyama cryptodome.

electrical currents into the ground at audio and near-audio frequencies via a grounded wire (dipole source), whilst a receiver records the electric field parallel to the grounded wire and the magnetic field perpendicular to the grounded wire (Fig. 4).

The CSAMT survey was carried out using a high-resolution electromagnetic system (Geo-SEM; Neoscience Co. Ltd, Osaka, Japan) consisting of a transmitter and a receiver (Fig. 5). The transmitter (Fig. 5A) comprises a transformer, rectifier, switching circuit, GPS clock, and generator. A grounded wire that is 1.5 km long with 25–35 electrodes at each termination was connected to the transmitter. The receiver (Fig. 5B) consists of an amplifier, filter, data logger, GPS clock, and set of sensors. The sensors are a pair of electrodes and a coil. The transmitter and receiver were synchronized with a high-precision quartz clock system using GPS to an accuracy of  $1 \times 10^{-6}$  s. The specifications of the Geo-SEM system are given in Table 1 and further details of the system are described in Johmori *et al.* (2010).

The transmitter was positioned 8.5 km south of the Showa–Shinzan Dome, with the 1.5-km-long grounded

wire oriented N67° W (Fig. 1). The survey line was 1600 m long and oriented N80° W (M1–12; Fig. 3). The 12 receiver stations (M1–12) were horizontally spaced at intervals of 65–225 m. The M1–2 and M12 receivers were located outside of the Showa–Shinzan Dome. The M3 and M6–11 receivers were located on the Yaneyama cryptodome, with the M6–10 receivers being located on the flat top of the cryptodome. The M4–5 receivers were located on the lava dome. The positions of the receiver stations were confirmed using GPS. The distance between the transmitter and receiver stations was 8.5 km (Fig. 1), which is 8.5 times larger than the depth of interest (1000 m), and sufficient to obtain CSAMT data in the far-field region beyond the near-field region (*e.g.*, Sandberg and Hohmann, 1982).

The CSAMT measurements were performed during 2–6 November 2012. The transmitter injected 1–8 A electrical currents into the ground at frequencies of 1, 2, 4, 8, 16, 32, 64, 128, 256, 512, 1024, 2048, 4096, and 8192 Hz, and another series at frequencies of 20, 40, 80, 160, 320, 640, 1280, 2560, and 5120 Hz, in order to minimize the noise related to the commercially used frequency of 50 Hz and its higher harmonics. The receiver recorded the electric and magnetic fields parallel (N67° W) and perpendicular, respectively, to the grounded wire. The measurement time at each receiver station was 1 h (2 min at 8192 Hz; 8 min at 1 Hz). The CSAMT data were then processed using a band-pass filter, a Fourier transform, and stacking to remove noise. The number of waves for stacking was  $> 400,000$  at 8192 Hz or  $> 300$  at 1 Hz. The apparent resistivity and phase were then calculated from the electric and magnetic fields. Measurement errors for the apparent resistivity and phase were not calculated, as frequency analyses for the CSAMT data were performed for a long time-series of data that was not divided into plural datasets, in order to increase the frequency resolution (see Johmori *et al.*, 2010).

The obtained CSAMT data comprising apparent resistivity and phase are shown in Fig. 6. The CSAMT data are inferred to have been measured in a far-field region that is beyond the near-field region, as: (1) the phase angles range from 30° to 65° at 1 Hz, with no angles of 0°; and (2) the apparent resistivity does not show abrupt V-shaped decreasing and increasing trends at low frequencies (*i.e.*, it does not show a ‘notch’ or ‘transition zone’; Hishida and Takasugi, 1998).

#### 4. Data analysis

The resistivity structure beneath the Showa–Shinzan Dome was calculated by 2D inversion of the CSAMT data using a finite element method, following Sasaki (1986). The 2D inversion was performed in transverse magnetic (TM) mode (Sasaki, 1986), along a section oriented N80° W and 1600 m in length (survey line; Fig. 3). The topographic model for the 2D inversion was obtained from 1 :

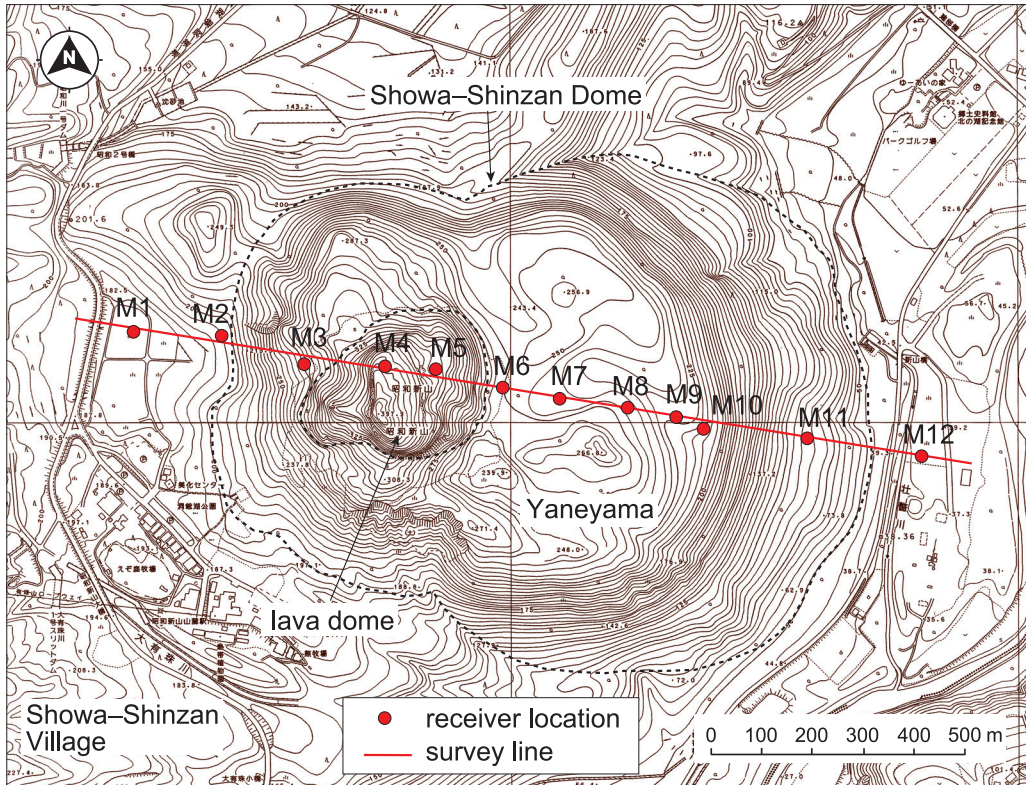


Fig. 3. Topographic map of the Showa-Shinzan Dome showing the survey line for the CSAMT survey (red line) and receiver stations (red circles; M1-12). The survey line is 1600 m long and oriented  $N80^\circ W$ . The base map was taken from the 1:5000 scale topographic maps 'Usuzan III' and 'Usuzan VI' issued by the Geospatial Information Authority of Japan. The topographic contour interval is 5 m.

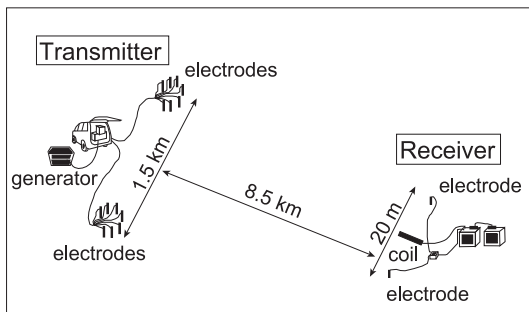


Fig. 4. Schematic of the electromagnetic system (GeoSEM) used for the CSAMT survey. The grounded wire for the transmitter is 1.5 km long and has 25–35 electrodes at each termination. The receiver has a set of sensors consisting of a pair of electrodes and a coil. The distance between the grounded wire and receiver stations is 8.5 km.

5000 scale topographic maps ('Usuzan III and VI') issued by the Geospatial Information Authority of Japan. The mesh size of the finite element method was 20 m (element size =  $20 \times 20$  m). Each inversion block representing the unit used to calculate resistivity by 2D inversion (Sasaki, 1986) consisted of four elements. The 2D inversion was carried out by comparing the field data (apparent resistivity and phase angles) with the calculated results using the non-linear least-squares method. The iteration for the 2D inversion was run eight times, using a uniform resistivity ( $25 \Omega \cdot m$ ) as the initial model. The value of  $25 \Omega \cdot m$  was determined from the average apparent resistivity at all the measurement locations. The effects of topography and static shift on the CSAMT data were reduced by 2D inversion. Static shift correction was not performed on the CSAMT data. Even if a near-surface resistivity anomaly was present, it was probably detected by the high-frequency CSAMT data (up to 8192 Hz) that were measured at closely spaced receiver stations (intervals 65–225 m), and therefore may not have caused distortion of the resistivity model (see Takasugi *et al.*, 1991).

Figure 6 compares the CSAMT field data (apparent

Table 1. Specifications of the exploration system used for the CSAMT survey (Geo SEM).

CSAMT survey system (Geo SEM)	
<b>Transmitter</b>	
Output power	5 kW (maximum)
Output voltage	1000 V (maximum)
Output current	10 A (maximum)
Frequency	1, 2, 4, 8, 16, 32, 64, 128, 256, 512, 1024, 2048, 4096, 8192 Hz
	20, 40, 80, 160, 320, 640, 1280, 2560, 5120 Hz
Generator	6 kW (maximum), 200V AC, 60 Hz, 3 phase
<b>Receiver</b>	
Frequency	1, 2, 4, 8, 16, 32, 64, 128, 256, 512, 1024, 2048, 4096, 8192 Hz
	20, 40, 80, 160, 320, 640, 1280, 2560, 5120 Hz
Channel	3 or 5 channels
Amplification degree	0–90 dB (10 dB pitch)
Wave analysis	stacking, Fourier transform

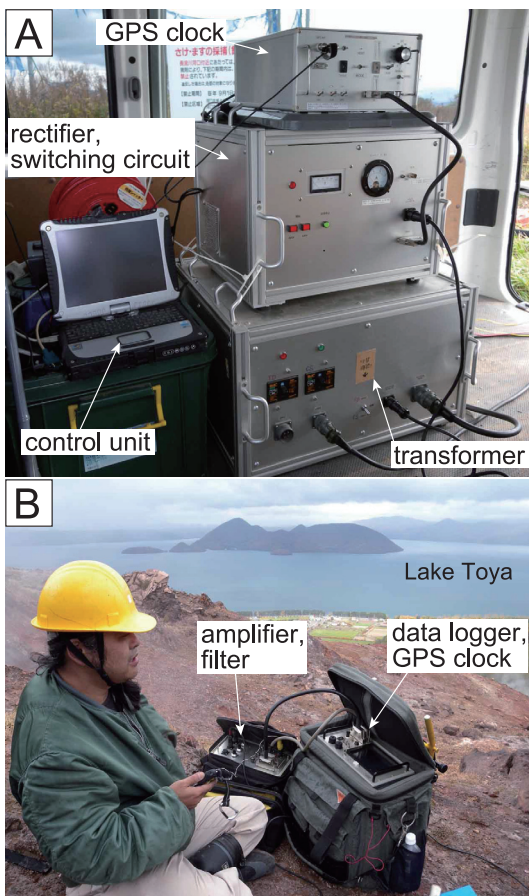


Fig. 5. Photographs of the transmitter (A) and receiver (B) of the electromagnetic system (Geo-SEM) used for the CSAMT survey. Photograph (B) was taken on the Showa–Shinzan Dome (receiver station M4; Fig. 3).

resistivity and phase angles) with the calculated 2D inversion results, showing good overall agreement. A root mean square (RMS) value was obtained from the field data (apparent resistivity) and the calculated results, in order to investigate quantitatively the match between the CSAMT field data and calculated results. The RMS value ( $\delta$ ) is defined as  $\delta = [\sum \{ \ln(\rho_{af}) - \ln(\rho_{ac}) \}^2 / n]^{1/2}$ , where  $\rho_{af}$  is the field measurement (apparent resistivity),  $\rho_{ac}$  is the calculated result, and  $n$  is the number of data ( $n = 276$ ). According to this definition, an RMS value equal to zero means that the calculated result perfectly matches the field data, whereas an RMS value equal to 0.1 means that almost 90% of the calculated result matches the field data (i.e., ~10% error). The obtained RMS value of 0.10 indicates good agreement between the field data and the calculated result.

The depth of penetration was determined from the skin depth (Cagniard, 1953). The skin depth is defined as the depth at which the amplitude of electromagnetic waves decreases to  $1/e$  (where  $e$  is the base of the natural logarithm). The skin depth calculated from the lowest-frequency electric currents (1 Hz) and its average apparent resistivity ( $5 \Omega \cdot \text{m}$ ) yields a penetration depth of 1100 m. The depth of penetration is thus *ca.* 1000 m below the ground surface.

## 5. Results and interpretation

Processing of the CSAMT data revealed the subsurface resistivity structure at depths of  $< 1000$  m beneath the Showa–Shinzan Dome (Fig. 7A). The resistivity structure is divided into four zones based on the resistivity values (zones A–D in Fig. 7B). In general, the resistivity of rocks and sediments is lowered by the presence of conductive minerals (*e.g.*, smectite-series clays), thermal waters in pores and fractures, and high temperatures (*e.g.*, Risk *et al.*, 2003). Geological interpretations of the four zones (A–D in Fig. 7B) are as follows.

Zone A, which has a resistivity of  $> 100 \Omega \cdot \text{m}$ , extends subhorizontally along the ground surface and is 50–100 m thick. This zone is present just below the surface of the

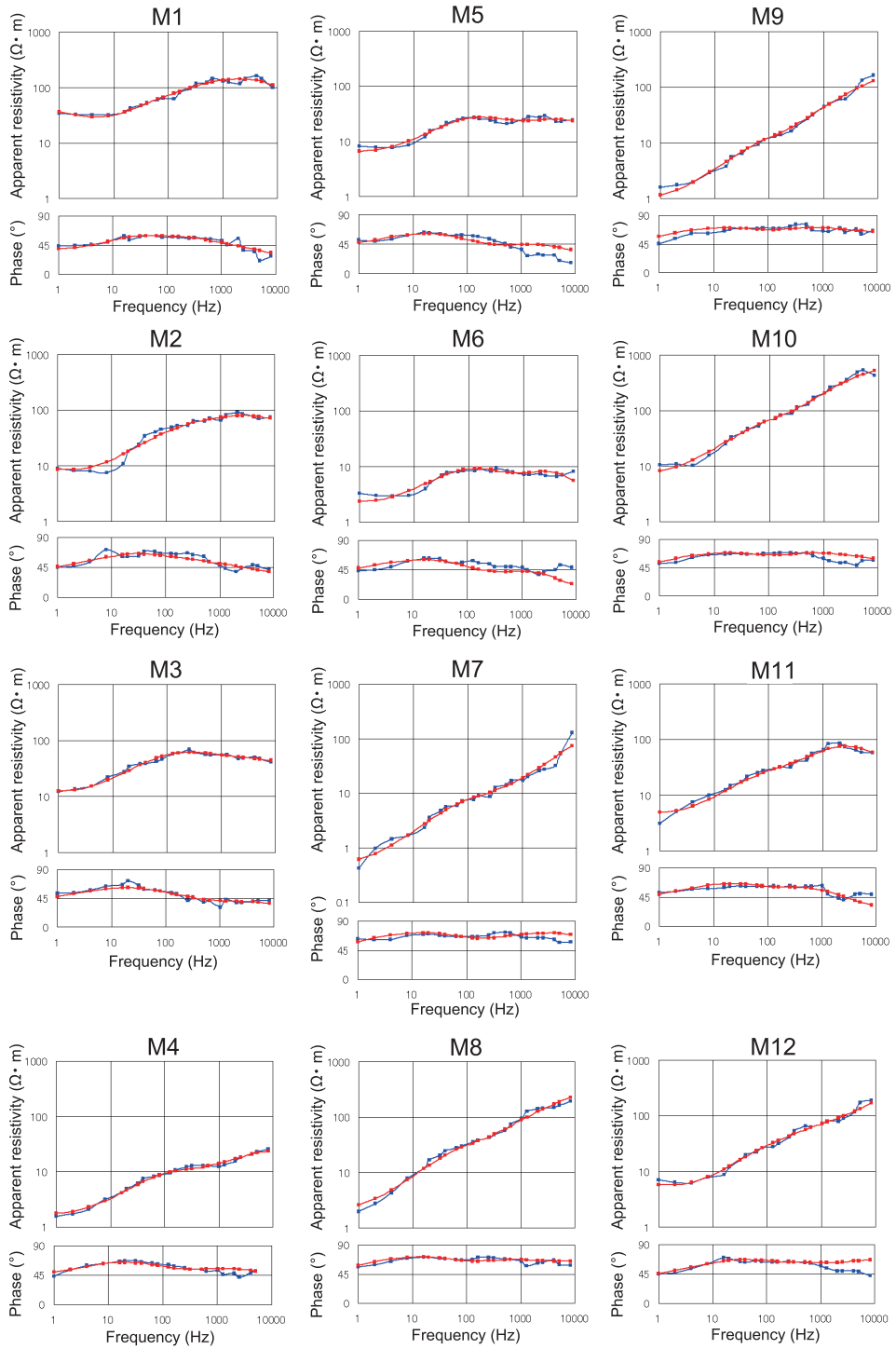


Fig. 6. Apparent resistivity and phase angles of the CSAMT field data (blue lines). Calculated 2D inversion results for the apparent resistivity and phase angles are also shown (red lines). Location numbers (M1–12) correspond to those shown in Fig. 3.

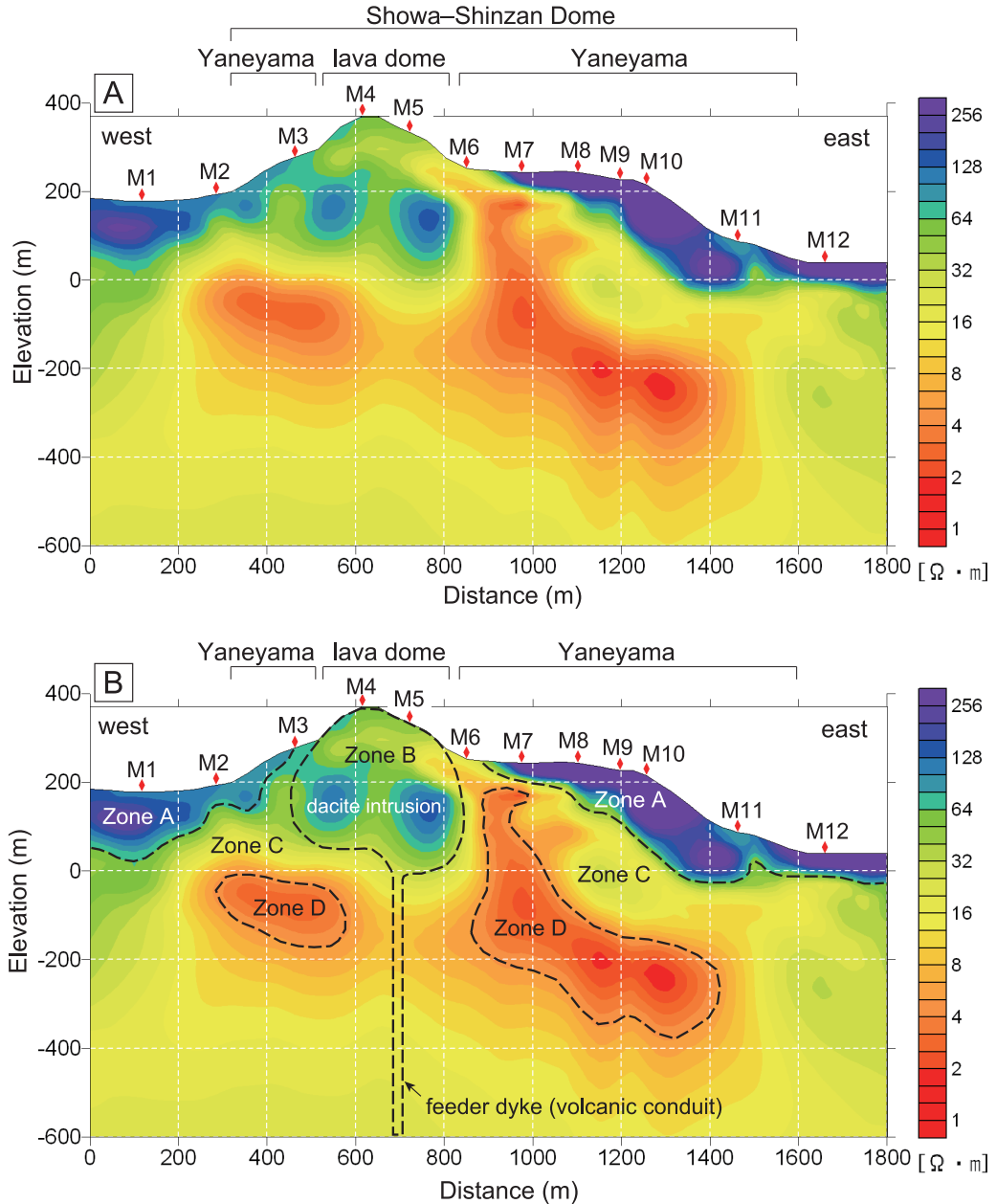


Fig. 7. Resistivity section beneath the Showa–Shinzan Dome (A) and its geological interpretation (B). Zone A is interpreted to represent andesitic lava blocks of the Usu Somma Lava. Zone B is inferred to be the dacite intrusion emplaced in AD 1943–45. Zone C (above zone D) is assigned to Quaternary pyroclastic flow deposits and sedimentary rocks, such as the Toya pyroclastic flow deposits, Fukaba Formation, Takinoue welded tuff, Sobetsu pumice flow deposits, and Yanagihara Formation. Zone D is inferred to be the Tertiary Osarugawa Formation, comprising intensely altered tuff breccia. The location and size of the feeder dyke is hypothetical.

Yaneyama cryptodome, but is absent at the lava dome. Given that the surface geology of the Yaneyama cryptodome is dominated by andesitic lava blocks of the Usu Somma Lava that were uplifted during the dome growth,

zone A is interpreted to represent these lava blocks. The absence of zone A at the lava dome may be attributed to lateral migration of the lava blocks from the lava dome area to the Yaneyama cryptodome area during extrusion of

the lava dome.

Zone B ( $50\text{--}130\ \Omega\cdot\text{m}$ ) is located below the summit of the Showa-Shinzan Dome and is a semi-circular domain that is  $\sim 400\text{ m}$  across in cross-section. Given that this zone is located immediately beneath the dacitic lava dome, we interpret it as a dacite intrusion within the Showa-Shinzan Dome (i.e., the dacite magma emplaced in AD 1943–45). Considering the emplacement age the Showa-Shinzan Dome, the dacite intrusion is probably solidified and not molten. However, the presence of active fumaroles on the lava dome suggests that the dacite intrusion is still at high temperatures. The intermediate resistivity ( $50\text{--}130\ \Omega\cdot\text{m}$ ) of zone B suggests that the dacite intrusion is partly hydrothermally altered. A fresh, unaltered dacite intrusion would have much higher resistivity (see Murase, 1962). We therefore infer that zone B represents a solidified high-temperature dacite intrusion that has been partly altered. The location and size of the dacite intrusion are consistent with the fact that active fumaroles occur on the lava dome and its immediate surrounds, but not on the Yaneyama cryptodome. The calculated volume of the dacite intrusion is  $3.3 \times 10^7\ \text{m}^3$ , assuming that the intrusion has a perfect spherical shape with a diameter of  $400\text{ m}$ .

Zone C ( $15\text{--}30\ \Omega\cdot\text{m}$ ) is located below zone A and occupies the interior of the Yaneyama cryptodome. The thickness of zone C (above zone D) is up to  $250\text{ m}$ . As zone A is interpreted to represent lava blocks of the Usu Somma Lava, zone C must be geological units underlying the Usu Somma Lava. The geological section of a borehole drilled  $1\text{ km}$  southwest of the Showa-Shinzan Dome (GS-R1 hole; length  $376\text{ m}$ ; Fig. 8) comprises the following units from base to top (Sato, 1967): the Tertiary Osarugawa Formation ( $36\text{ m}$  of intensely altered tuff breccia), the Quaternary Yanagihara Formation ( $121\text{ m}$  of volcanic sandstone), the Sobetsu pumice flow deposits ( $9\text{ m}$  of dacitic pumice), the Takinoue welded tuff ( $57\text{ m}$  of densely welded pumice), the Fukaba Formation ( $11\text{ m}$  of conglomerate), the Toya pyroclastic flow deposits ( $59\text{ m}$  of rhyolitic pumice), the Usu Somma Lava ( $72\text{ m}$  of andesite lava), and volcanic ash ( $11\text{ m}$ ). Given that the lowermost Tertiary Osarugawa Formation corresponds to zone D (described later), zone C (thickness  $<250\text{ m}$ ) is interpreted to represent the sequence from the Yanagihara Formation through to the Toya pyroclastic flow deposits. The low resistivity of zone C ( $15\text{--}30\ \Omega\cdot\text{m}$ ) suggests that these Quaternary pyroclastic deposits and sedimentary rocks are hydrothermally altered. The thickness variations of Zone C (Fig. 7) imply that these pyroclastic deposits and sedimentary rocks are highly deformed. We are unable to infer the nature of the deeper part of zone C (below zone D), as there are no drilling data at depths of  $>376\text{ m}$  below ground level (Sato, 1967).

Zone D ( $<5\ \Omega\cdot\text{m}$ ) is present  $300\text{--}400\text{ m}$  below the Showa-Shinzan Dome and is  $\sim 200\text{ m}$  thick. This zone extends subhorizontally but branches upwards below the

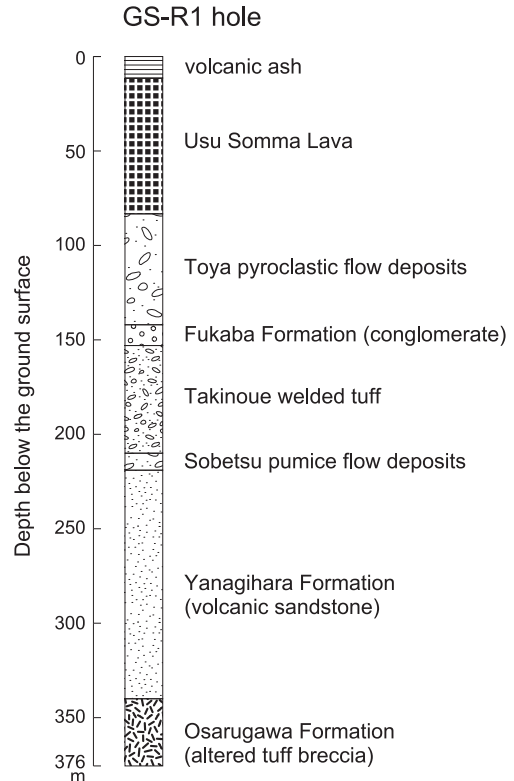


Fig. 8. Stratigraphic section of the GS-R1 hole drilled  $1\text{ km}$  southwest of the Showa-Shinzan Dome (see Fig. 1). Modified from Sato (1967).

M7 receiver location (Fig. 7B). Zone D is characterized by extremely low resistivity and is interpreted to be altered pyroclastic deposits containing abundant conductive clay minerals such as smectite. Other interpretations, such as the presence of thermal waters or high temperatures, cannot readily explain the location and shape of zone D. Considering the depth of zone D ( $300\text{--}400\text{ m}$ ) and the geology of the GS-R1 drillhole (Fig. 8; Sato, 1967), zone D is interpreted to be the Tertiary Osarugawa Formation (intensely altered tuff breccia) that contains abundant clay minerals (Oshima and Matsushima, 1999; Takakura *et al.*, 2009). We attribute the upward branching of zone D below M7 (Fig. 7B) to lateral displacement (i.e., eastward migration) and uplift of the Osarugawa Formation that resulted from emplacement of the dacite intrusion. Uplift of the Tertiary Osarugawa Formation is consistent with the local exposure of the Takinoue welded tuff and Fukaba Formation (i.e., the units underlying the Usu Somma Lava; Fig. 8) in a small area ( $100 \times 150\text{ m}$ ) on the Yaneyama cryptodome in the regions around the M6–7 receivers (Nemoto *et al.*, 1957).

## 6. Discussion

Previous studies have proposed various models for the subsurface geological structure of the Showa-Shinzan Dome. Nakamura and Mori (1949) carried out laboratory analog modeling experiments of the Showa-Shinzan Dome using sand and iron rods, and concluded that the morphology of the dome could be explained by the ascent of a cylindrical dacite intrusion (~300 m across) beneath the lava dome, and another, smaller, cylindrical dacite intrusion beneath the Yaneyama cryptodome. Hayakawa *et al.* (1957) conducted a seismological study of the Showa-Shinzan Dome and inferred the existence of a dacite intrusion located beneath the dome that extends laterally to the deeper part of the Yaneyama cryptodome. Nishida and Miyajima (1984) conducted a magnetic survey over Usu Volcano, including Showa-Shinzan Dome, and inferred the existence of a dacite intrusion 400 m across beneath the lava dome. Nishida and Miyajima (1984) also invoked the presence of another dacite intrusion beneath the Yaneyama cryptodome, following the model of Nakamura and Mori (1949). Symonds *et al.* (1996) considered that the sizeable uplift associated with the Yaneyama cryptodome represents the large volume of magma intruded beneath the cryptodome, and proposed a model in which a large dacite intrusion occupies the interior of the cryptodome. The study of Hernandez *et al.* (2006) adopted the model of Symonds *et al.* (1996). Tanaka and Yokoyama (2008) performed a muon radiography survey of the Showa-Shinzan Dome and proposed that the lava dome decreases in diameter downward, and grades into a volcanic conduit with a diameter of  $100 \pm 15$  m at 260 m above sea level and  $50 \pm 15$  m at 217 m above sea level.

Our model is characterized by the existence of a sub-spherical dacite intrusion (~400 m across) beneath the lava dome, and the absence of a dacite intrusion beneath the Yaneyama cryptodome (Fig. 7B). This model differs from the previous models described above, in terms of the location and size of the dacite intrusion. We discount the possible existence of a dacite intrusion beneath the Yaneyama cryptodome, as the interior of the cryptodome is characterized by low resistivity (Fig. 7). Our model can also readily explain the spatial distribution of active fumaroles, which occur on the lava dome and its surroundings, but not on the Yaneyama cryptodome. We consider that the Yaneyama cryptodome formed by uplift and lateral migration of pre-existing rocks and sediments due to the intrusion of dacite magma. Such a formation mechanism is consistent with the growth history of the Showa-Shinzan Dome (Mimatsu, 1962).

## 7. Conclusions

A CSAMT survey has revealed the subsurface resistivity structure at depths of <1000 m beneath the Showa-Shinzan Dome. The obtained resistivity structure suggests the presence of a sub-spherical dacite intrusion that is ~400

m across, representing solidified magma emplaced beneath the lava dome in AD 1943–45. The Yaneyama cryptodome only comprises pre-existing rocks and sediments uplifted by the intrusion of dacitic magma and is not underlain by a dacite intrusion.

## Acknowledgements

This research was financially supported by the Muroran Institute of Technology. S. Mimatsu (Mimatsu Masao Memorial Hall) is thanked for allowing our field survey of the Showa-Shinzan Dome. We thank T. Takahashi (Neo Science) for assistance in the field. Y. Nishida (Hokkaido University) is thanked for constructive discussions about the internal structure of the Showa-Shinzan Dome. Comments by two anonymous referees and T. Hashimoto (Hokkaido University) significantly improved the manuscript.

## References

- Aizawa, K. (2010) Groundwater flow beneath volcanoes inferred from electric self-potential and magnetotellurics. *Bull. Volcanol. Soc. Japan*, **55**, 251–259. (in Japanese)
- Aizawa, K., Ogawa, Y., Hashimoto, T., Koyama, T., Kanda, W., Yamaya, Y., Mishina, M. and Kagiya, T. (2008) Shallow resistivity structure of Asama volcano and its implications for magma ascent process in the 2004 eruption. *J. Volcanol. Geotherm. Res.* **173**, 165–177.
- Aizawa, K., Ogawa, Y. and Ishido, T. (2009) Groundwater flow and hydrothermal systems within volcanic edifices: Delineation by electric self-potential and magnetotellurics. *J. Geophys. Res.*, **114**, doi: B0120810.1029/2008jb005910.
- Cagniard, L. (1953) Basic theory of the magneto-telluric method of geophysical prospecting. *Geophysics*, **18**, 605–635.
- Fikos, I., Vargemezis, G., Zlotnicki, J., Puertollano, J.R., Alanis, P.B., Pigtain, R.C., Villacorte, E.U., Malipot, G.A. and Sasai, Y. (2012) Electrical resistivity tomography study of Taal volcano hydrothermal system, Philippines. *Bull. Volcanol.*, **74**, 1821–1831.
- Hayakawa, M., Matsuda, T., Mori, K., Obi, N., Otaki, T., Furuya, S., Murauchi, S., Kubotera, A., Iwasaki, S., Sano, S., Kanai, M., Saito, T., Sakuma, S. and Hasegawa, H. (1957) Prospecting of the underground structure of “Showa-Shinzan” by various geophysical methods, particularly seismic survey. *Japan J. Geophys.* **1**, 13–20.
- Hernandez, P.A., Notsu, K., Okada, H., Mori, T., Sato, M., Barahona, F. and Perez, N.M. (2006) Diffuse emission of CO<sub>2</sub> from Showa-Shinzan, Hokkaido, Japan: a sign of volcanic dome degassing. *Pure Appl. Geophys.*, **163**, 869–881.
- Hishida, H. and Takasugi, S. (1998) The CSAMT method. In *Handbook for geophysical exploration* (Society of Exploration Geophysics of Japan ed.), 322–325, Society of Exploration Geophysics of Japan. (in Japanese)
- Johmori, A., Mitsuhata, Y., Nishimura, S., Johmori, N., Kondou, T. and Takahashi, T. (2010) Development of a deep electro-

- magnetic exploration instrument with high frequency spectrum resolution using GPS synchronization. *J. Japan Soc. Engin. Geol.*, **51**, 62–72. (in Japanese with English abstract)
- Kato, Y. and Shoji, R. (1949) Determination of the underground structure of the new volcano of Mt. Showa by the seismic prospecting. *Sci. Rep. Tohoku Univ., Ser. 5*, **1**, 41–44.
- Katsui, Y. (1988) Usu Volcano, its evolution and eruptive history. In *1977–82 volcanism and environmental hazards of Usu Volcano* (Kadomura, H., Okada, H. and Araya, T. eds.), 225–234, Hokkaido University Press, Sapporo. (in Japanese)
- Matsuoka, T. (2005) **Dictionary of exploration geophysics.** Society of Exploration Geophysics of Japan ed., Aichi Shuppan, Tokyo, 279p. (in Japanese)
- Matsushima, N., Oshima, H., Ogawa, Y., Takakura, S., Satoh, H., Utsugi, M. and Nishida, Y. (2001) Magma prospecting in Usu volcano, Hokkaido, Japan, using magnetotelluric soundings. *J. Volcanol. Geotherm. Res.* **109**, 263–277.
- Milsom, J. (2003) **Field Geophysics.** John Wiley and Sons, England, 232p.
- Mimatsu, M. (1962) **Showa-Shinzan diary.** Mimatsu Masao Memorial Hall, Sobetsu, Hokkaido, 225p. (in Japanese)
- Minakami, T., Ishikawa, T. and Yagi, K. (1951) The 1944 eruption of Volcano Usu in Hokkaido, Japan. *Bull. Volcanol.*, **11**, 45–157.
- Murase, T. (1962) Viscosity and related properties of volcanic rocks at 800° to 1400°C. *J. Fac. Sci., Hokkaido Univ., Ser. VII*, **1**, 487–584.
- Nakamura, S. and Mori, T. (1949) On the mechanism of the formation of the Showa New Mountain of Usu volcano, Hokkaido, Japan. *Sci. Rep. Tohoku Univ. Ser. 5*, **1**, 45–49.
- Nemoto, T., Hayakawa, M., Takahashi, K. and Oana, S. (1957) Report on the geological, geophysical, and geochemical studies of Usu volcano (Showashinzan). *Rep. Geol. Surv. Japan*, **170**, 1–149. (in Japanese with English abstract)
- Nishida, Y. and Miyajima, E. (1984) Subsurface structure of Usu volcano, Japan as revealed by detailed magnetic survey. *J. Volcanol. Geotherm. Res.* **22**, 271–285.
- Nishida, Y., Utsugi, M., Oshima, H., Kagiya, T., Inoue, T., Morita, Y., Shigehara, S. and Maekawa, T. (1996) Resistivity structure of Usu volcano as revealed by the magnetotelluric measurements. *Geophys. Bull. Hokkaido Univ.*, **59**, 151–162. (in Japanese with English abstract)
- Oba, Y., Katsui, Y., Kurasawa, H., Ikeda, Y. and Uda, T. (1983) Petrology of historic rhyolite and dacite from Usu volcano, north Japan. *J. Fac. Sci., Hokkaido Univ., Ser. IV*, **20**, 275–290.
- Ogawa, Y., Matsushima, N., Oshima, H., Takakura, S., Utsugi, M., Hirano, K., Igarashi, M. and Doi, T. (1998) A resistivity cross-section of Usu volcano, Hokkaido, Japan, by audiomagnetotelluric soundings. *Earth Planets Space*, **50**, 339–346.
- Oshima, H. and Matsushima, N. (1999) Preliminary report on hydrological environment in the shallow part of Usu volcano. *Geophys. Bull. Hokkaido Univ.*, **62**, 79–97. (in Japanese with English abstract)
- Risk, G.F., Caldwell, T.G. and Bibby, H.M. (2003) Tensor time domain electromagnetic resistivity measurements at Ngatamariki geothermal field, New Zealand. *J. Volcanol. Geotherm. Res.* **127**, 33–54.
- Sandberg, S.K. and Hohmann, G.W. (1982) Controlled-source audiomagnetotellurics in geothermal exploration. *Geophysics*, **47**, 100–116.
- Sasaki, Y. (1986) Resolving power of MT method for two-dimensional structures. *Butsuri-Tansa*, **39**, No. 4, 1–9. (in Japanese with English abstract)
- Sato, H. (1967) Drill cores from Showa-Shinzan Research Geothermal Well GS-R1. *Abst. Geol. Surv. Japan, Hokkaido branch*, No. 18, 24–27. (in Japanese)
- Soya, T., Katsui, Y., Niida, K., Sakai, K. and Tomiya, A. (2007) **Geological map of Usu Volcano (2<sup>nd</sup> edition).** Geological survey of Japan, AIST, Tsukuba.
- Srigitomo, W., Kagiya, T., Kanda, W., Munekane, H., Hashimoto, T., Tanaka, Y., Utada, H. and Utsugi, M. (2008) Resistivity structure of Unzen volcano derived from time domain electromagnetic (TDEM) survey. *J. Volcanol. Geotherm. Res.* **175**, 231–240.
- Symonds, R.B., Mizutani, Y. and Briggs, P.H. (1996) Long-term geochemical surveillance of fumaroles at Showa-Shinzan dome, Usu volcano, Japan. *J. Volcanol. Geotherm. Res.* **73**, 177–211.
- Takakura, S., Hashimoto, T., Ogawa, Y., Inoue, H., Yamaya, Y., Ichihara, H., Mogi, T., Utsugi, M., Matsushima, N. and Satoh, H. (2009) Magnetotelluric investigations along the eastern foot of Usu Volcano. *Geophys. Bull. Hokkaido Univ.*, **72**, 107–115. (in Japanese with English abstract)
- Takasugi, S., Kawakami, N. and Muramatsu, S. (1991) Reduction of the static effect in magnetotellurics using audio-frequency MT data. *Butsuri-Tansa*, **45**, No. 2, 116–128.
- Tanaka, H.K.M. and Yokoyama, I. (2008) Muon radiography and deformation analysis of the lava dome formed by the 1944 eruption of Usu, Hokkaido -contact between high-energy physics and volcano physics-. *Proc. Jpn. Acad. Ser. B*, **84**, 107–116.
- Tanaka, H. K. M., Nakano, T., Takahashi, S., Yoshida, J., Ohshima, H., Maekawa, T., Watanabe, H. and Niwa, K. (2007) Imaging the conduit size of the dome with cosmic-ray muons: the structure beneath Showa-Shinzan lava dome, Japan. *Geophys. Res. Lett.*, **34**, doi: 10.1029/2007GL031389.
- Yamaya, Y., Mogi, T., Hashimoto, T. and Ichihara, H. (2009) Hydrothermal system beneath the crater of Tarumai volcano, Japan: a 3-D resistivity structure revealed using audio-magnetotellurics and induction vector. *J. Volcanol. Geotherm. Res.* **187**, 193–202.
- Yokokawa, K. (1984) Outline of CSAMT survey. *Butsuri-Tansa*, **37**, No. 5, 61–68. (in Japanese)
- Yokoyama, I., Katsui, Y., Oba, Y. and Ehara, Y. (1973) **Usuzan, its volcanic geology, history of eruption, present state of activity and prevention of disasters.** Committee for Prevention and Disasters of Hokkaido, Sapporo, 254 p. (in Japanese)

(Editorial handling Takechi Hashimoto)

## 北海道有珠火山，昭和新山ドームの比抵抗構造

後藤芳彦・城森 明

北海道南西部，有珠火山東部に位置する昭和新山は，1943-1945年の噴火で形成され，屋根山と呼ばれる扁平な潜在ドームと，ピラミッド型の溶岩ドームからなる。昭和新山の内部構造を解明するため，CSAMT法による比抵抗構造探査（深度<1000m）を行った。探査は昭和新山を東西方向に横断する測線上（測線長1600m，受信点12箇所）で行い，データ解析は有限要素法を用いた2次元逆解析で行った。その結果，溶岩ドーム直下に，直径約400mのデイサイト貫入岩体が存在することが明らかになった。この貫入岩体は1943-1945年に貫入したマグマが固結したものであると考えられる。屋根山はデイサイト貫入岩体により押し上げられた既存の岩石や堆積物（有珠外輪山溶岩，洞爺火砕流堆積物など）からなり，屋根山内部にデイサイト貫入岩体は存在しない。